Synergy of Observations and Dynamo Models to Understand and Predict Solar Activity Cycles

Irina N. Kitiashvili

NASA Ames Research Center, BAERI

The long-standing problem of understanding the evolution of the global magnetic fields that drive solar activity through different temporal scales is becoming more tractable because, in addition to 400 years of sunspot records, we now have almost 4 solar cycles of magnetic field observations. These observations allow us to discern physical connections between dynamo model variables and observations using data assimilation analysis. In particular, the Ensemble Kalman Filter approach takes into account uncertainties in both observations and modeling and allows us to make reliable forecasts of solar cycle activity by using a relatively simple non-linear dynamical model of the solar dynamo. To expand this approach for more complex 2D and 3D dynamo modeling, it is necessary to decompose the observed synoptic magnetograms into poloidal and toroidal field components. In this presentation I will present initial results on magnetogram decomposition and assimilation of magnetogram data into dynamo modeling.

Data Assimilation Methodology

Observations

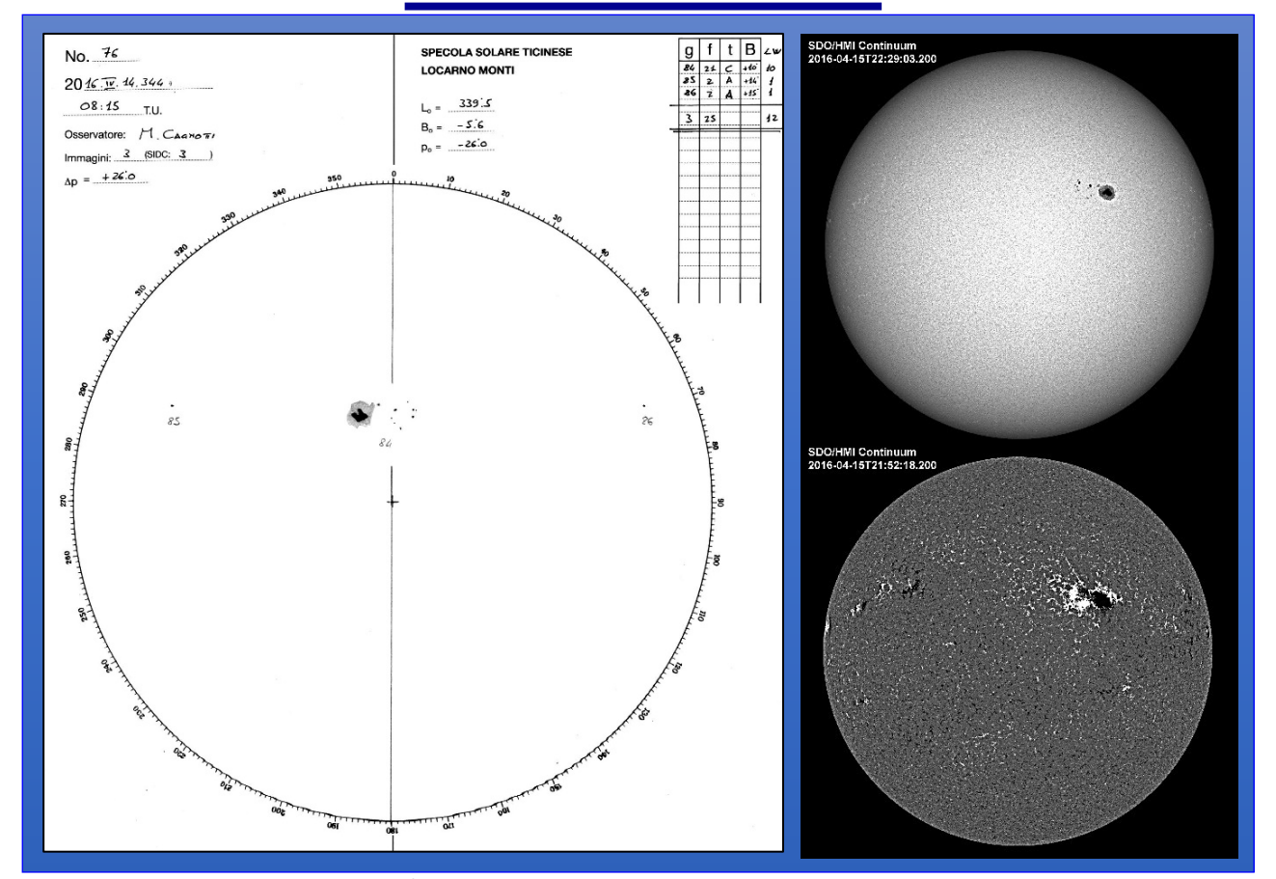

Dynamo model

Parker 1955, Kleeorin & Ruzmaikin, 1982
Kitiashvili & Kosovichev 2009, 2011

$$\frac{\partial A}{\partial t} = \alpha B + \eta \nabla^2 A \qquad \alpha_k = -(\tau/3)\langle \mathbf{u}(\nabla \times \mathbf{u})\rangle$$

$$\frac{\partial B}{\partial t} = G\frac{\partial A}{\partial z} + \eta \nabla^2 B \qquad \alpha_m = (\tau/12\pi\rho)\langle \mathrm{h}(\nabla \times \mathrm{h})\rangle$$

$$\alpha = \alpha_k + \alpha_m$$

$$\frac{\partial \alpha_m}{\partial t} = \frac{\mu}{4\pi\rho}\left(\mathbf{B}\cdot(\nabla\times\mathbf{B}) - \frac{\alpha \mathbf{B}^2}{\eta}\right) - \frac{\alpha_m}{T_\alpha}$$

$$\underbrace{d_j = \psi^t + \varepsilon_j \qquad j = 1,\dots,N \qquad\qquad d\psi = G(\psi)dt + h(\psi)dq}_{}$$

Kalman gain

$$K_e = \frac{\left(C^e_{\psi\psi}\right)^f M^T}{M\left(C^e_{\psi\psi}\right)^f M^T + C^e_{\varepsilon\varepsilon}}$$

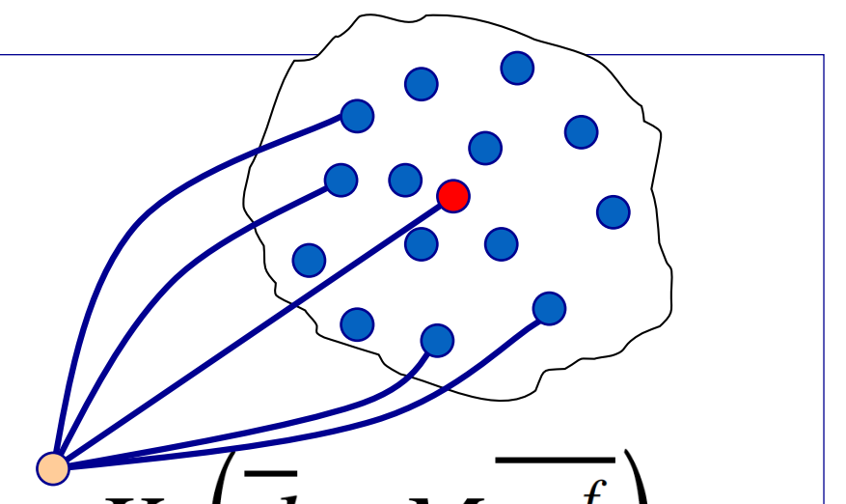

$$\psi^a_j = \psi^f_j + K_e\left(d_j - M\psi^f_j\right) \qquad \overline{\psi^a} = \overline{\psi^f} + K_e\left(\overline{d} - M\overline{\psi^f}\right)$$

$$\psi^a_j - \overline{\psi^a} = (I - K_e M)\left(\psi^f_j - \overline{\psi^f}\right) + K_e\left(d_j - \overline{d}\right)$$

$$\left(C^e_{\psi\psi}\right)^a = \overline{\left(\psi^a_j - \overline{\psi^a}\right)\left(\psi^a_j - \overline{\psi^a}\right)^T} = (I - K_e M)\left(C^e_{\psi\psi}\right)^f$$

Synoptic magnetogram. The color scale is saturated at +/-15G. The yellow dashed lines indicate different moments of time: 1992 and 2015.

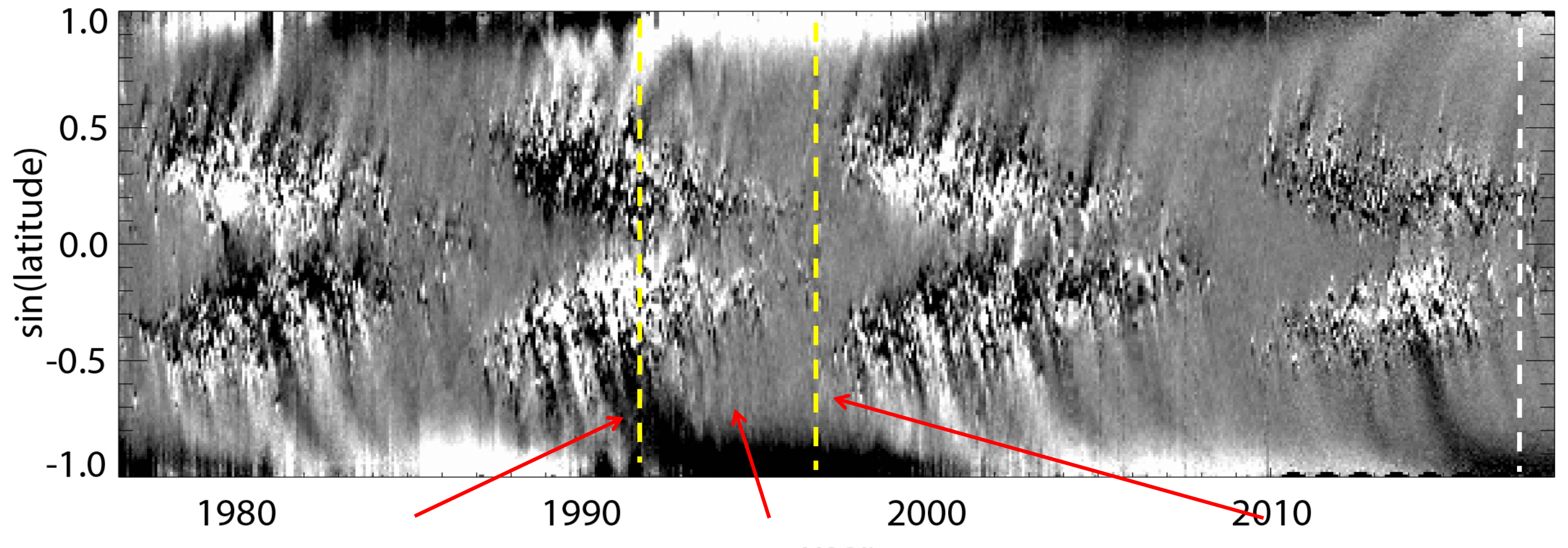

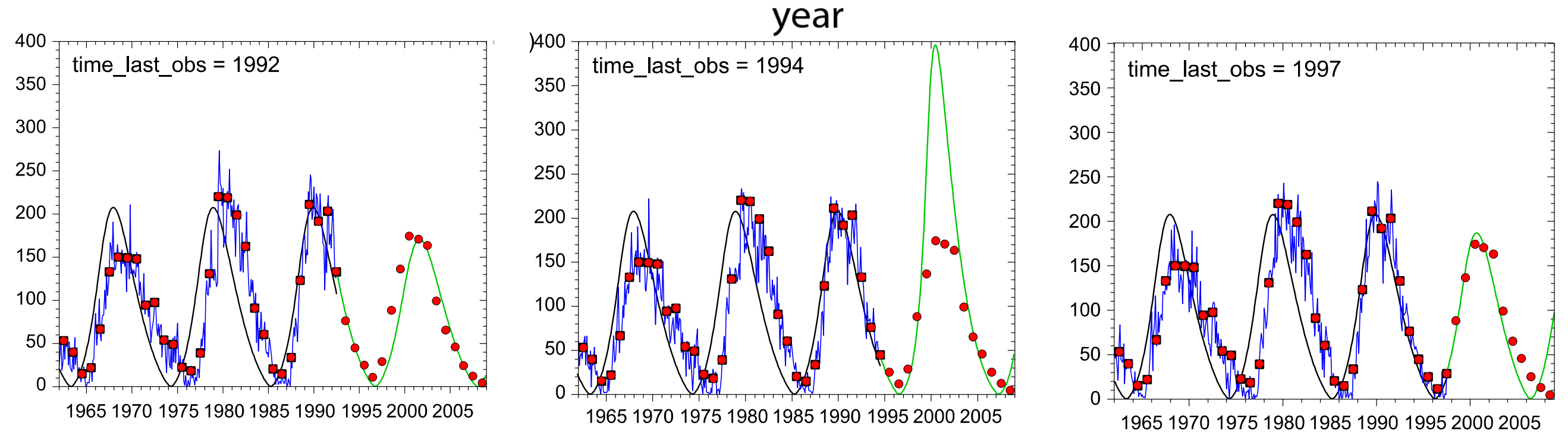

Comparison of sunspot number predictions and estimated parameters at the solar minima

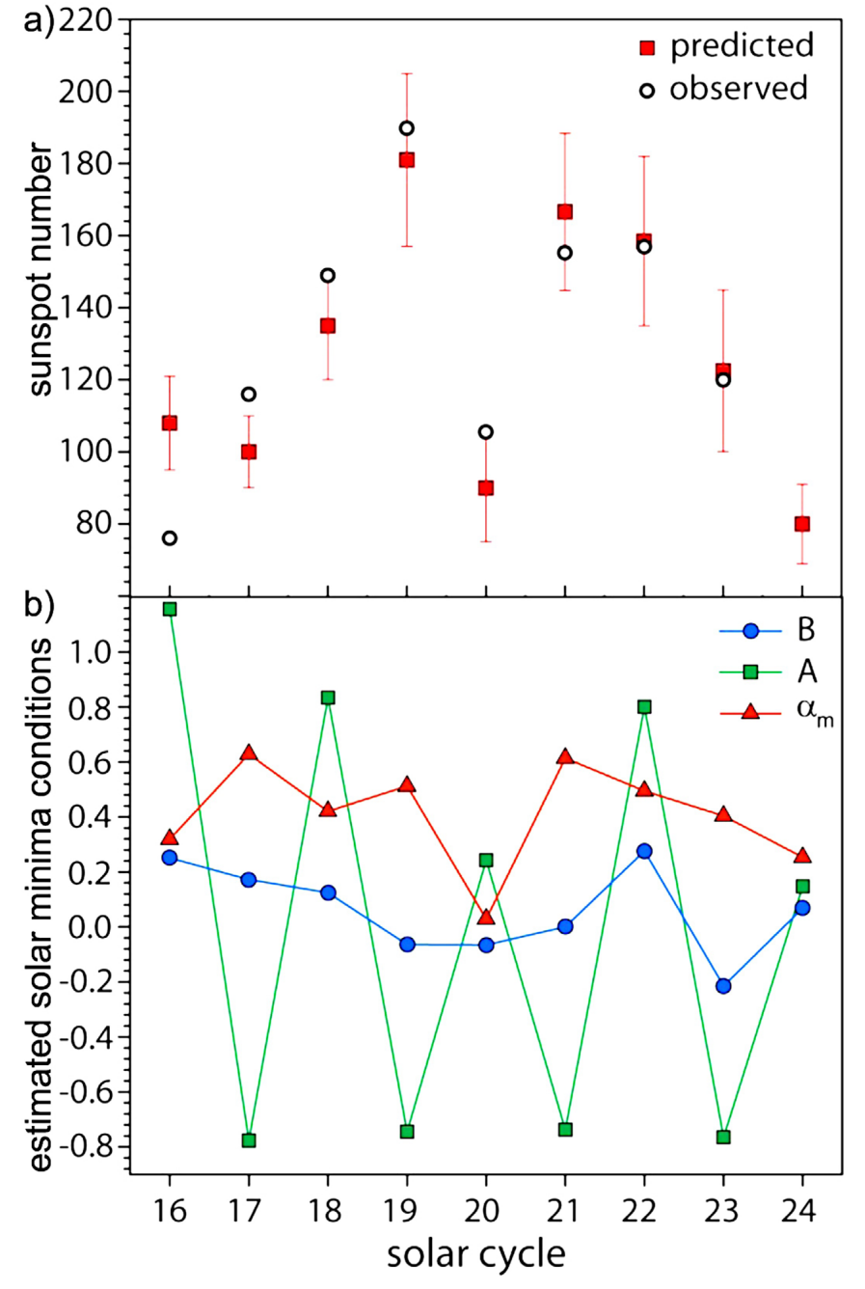

Toroidal magnetic field does not show a particular pattern and is close to zero.

Vector-potential of the poloidal field changes sign corresponding to the polar field reversal. The amplitude at the start of cycles 20 and 24 is substantially lower than during other minima.

This may correspond to the well-known correlation between the strength of the polar magnetic field and the following sunspot number (Schatten 2005; Svalgaard et al, 2005)

The large-scale magnetic helicity shows significantly better correlation with future sunspot numbers; in particular, the magnetic helicity substantially decreases prior to weak sunspot cycles.

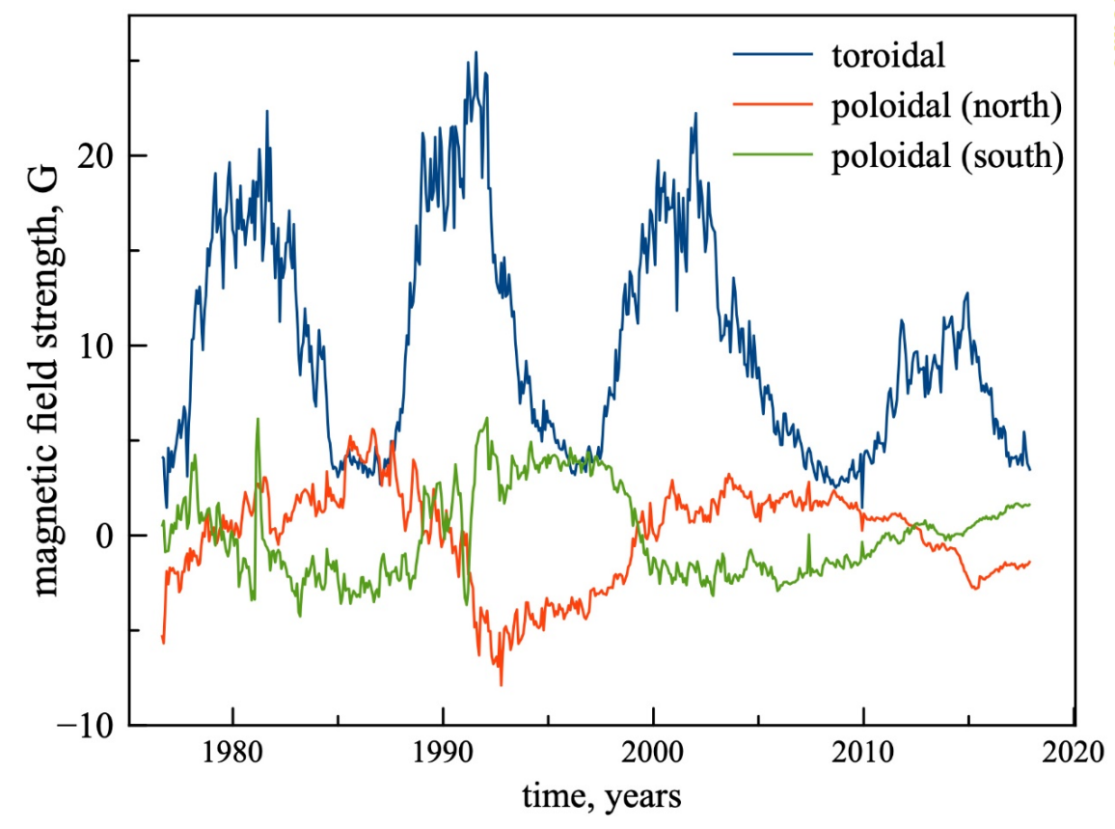

Results of magnetic field decomposition into toroidal and poloidal field components from the observed radial field synoptic magnetograms.

Effect of the Ensemble Kalman Filter Parameters on predictive capabilities of Solar Cycles

Solar Cycle 23 prediction:

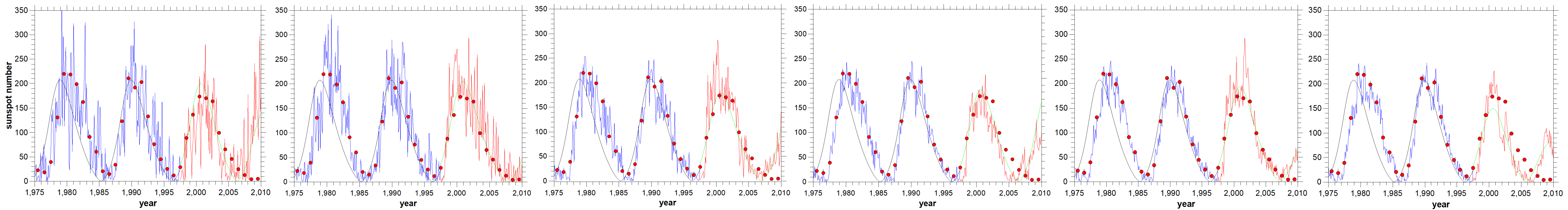

Solar Cycle 19 prediction:

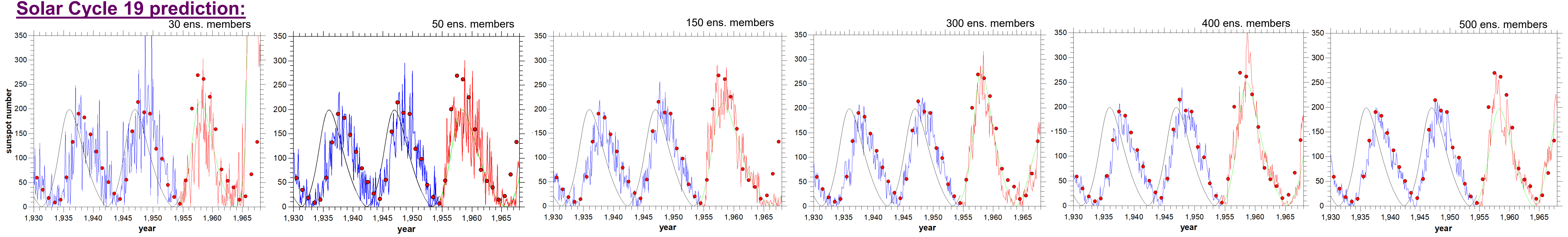

Test predictions of Solar Cycles 23 (top row) and 19 (bottom) reveal the influence of the number of ensemble members on the ability of the dynamo model to predict future activity cycles.

Discrepancies between the model solutions and observational data for Solar Cycles 10 - 18, and synthetic data generated for different numbers of ensemble members in test cases of the prediction for Solar Cycle 19.

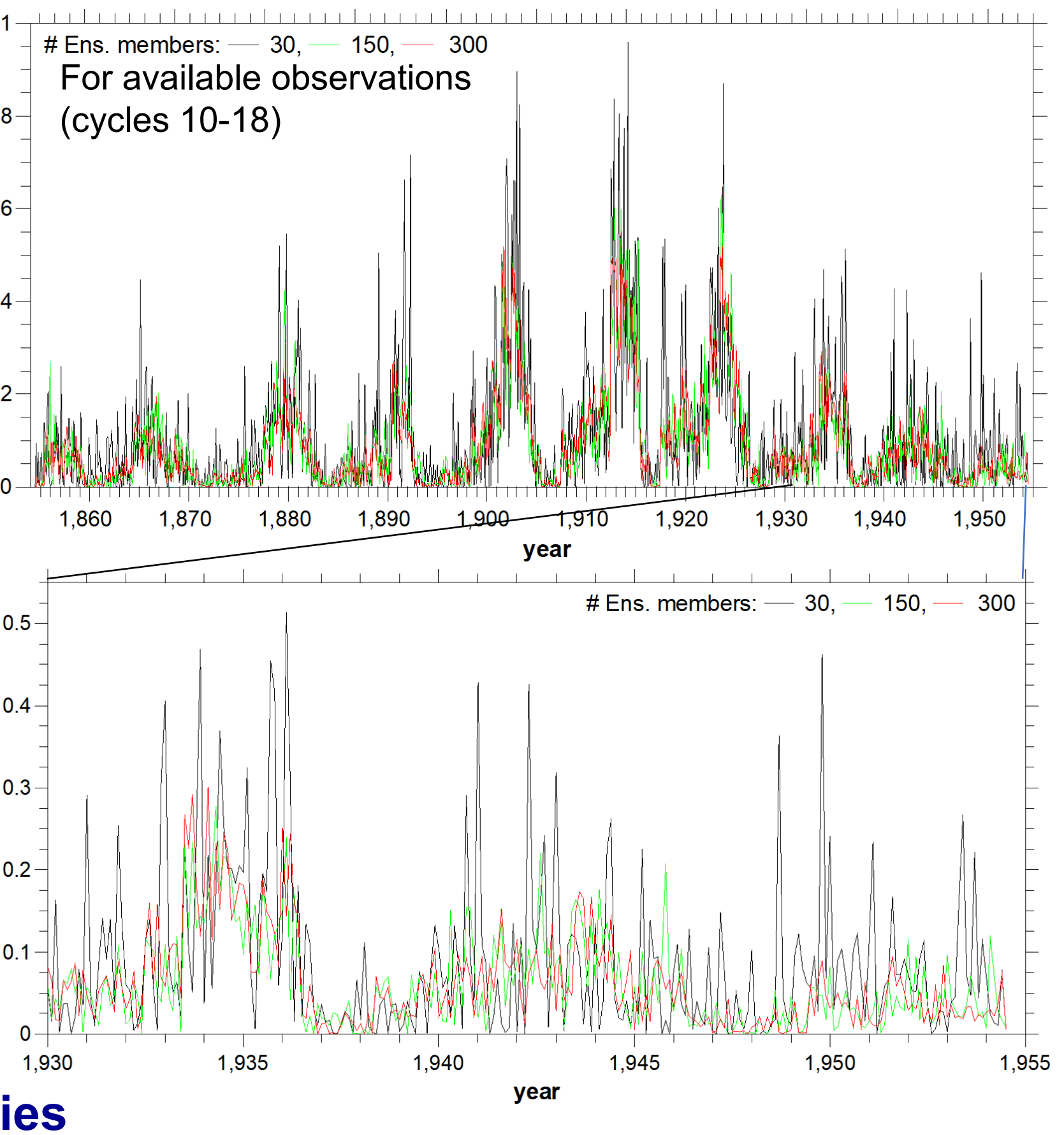

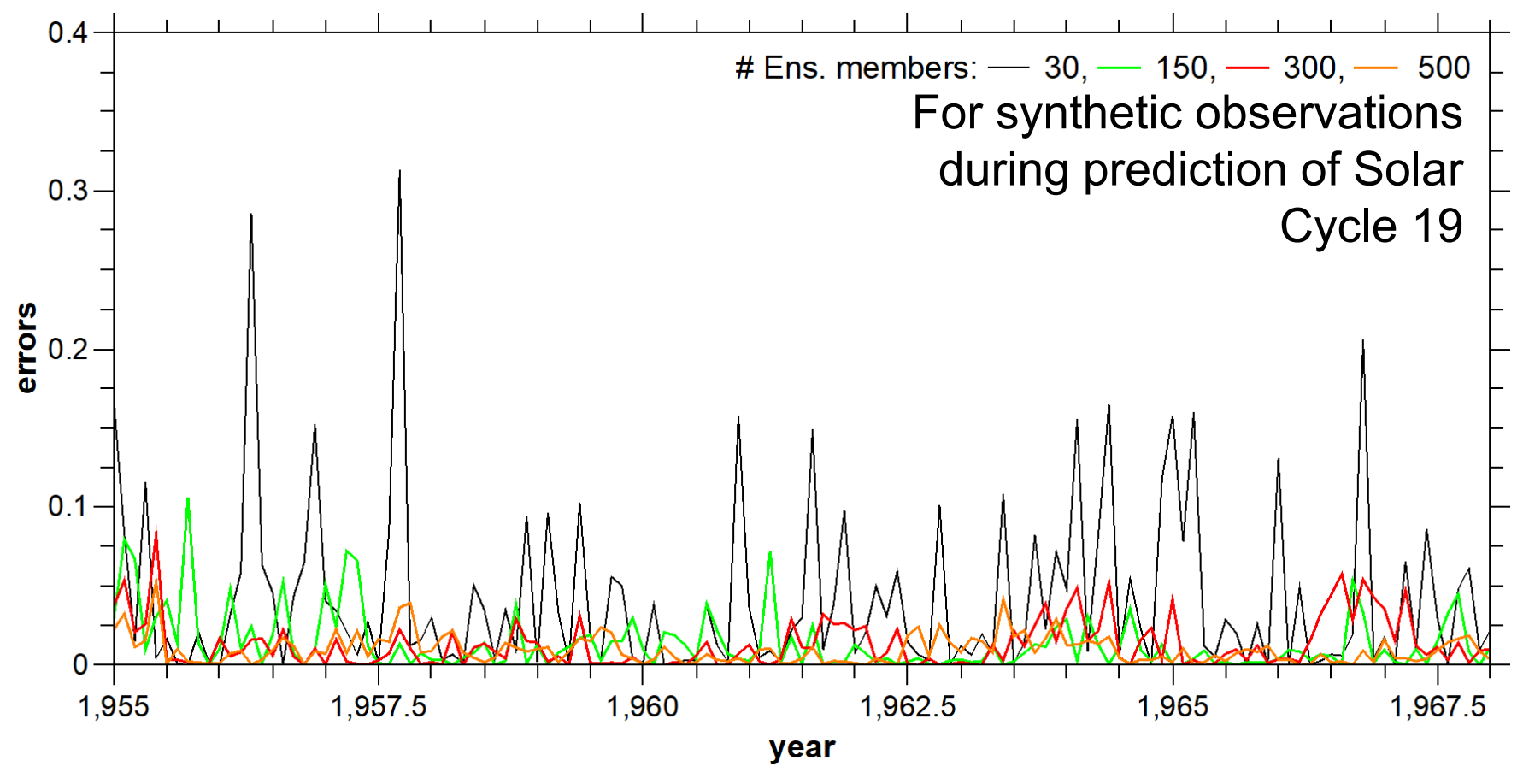

Early estimation of properties of Solar Cycle 25 (for the sunspot number version 2.0) shows 1) prediction obtained for observations which include the sunspot number data up to the solar minimum in 2008 (green curve); 2) prediction obtained for the last observation during the polar magnetic field reversal (purple/violet); 3) prediction obtained using all currently available observations up to 2017 (red curve). Blue curve shows the best EnKF estimates of the previous cycles based on the dynamo model (4) and all available sunspot observations (red circles).

Comparison of best estimates of the sunspot number variations according to the annual sunspot numbers (blue curves), future observations (red curve), and monthly sunspot numbers.

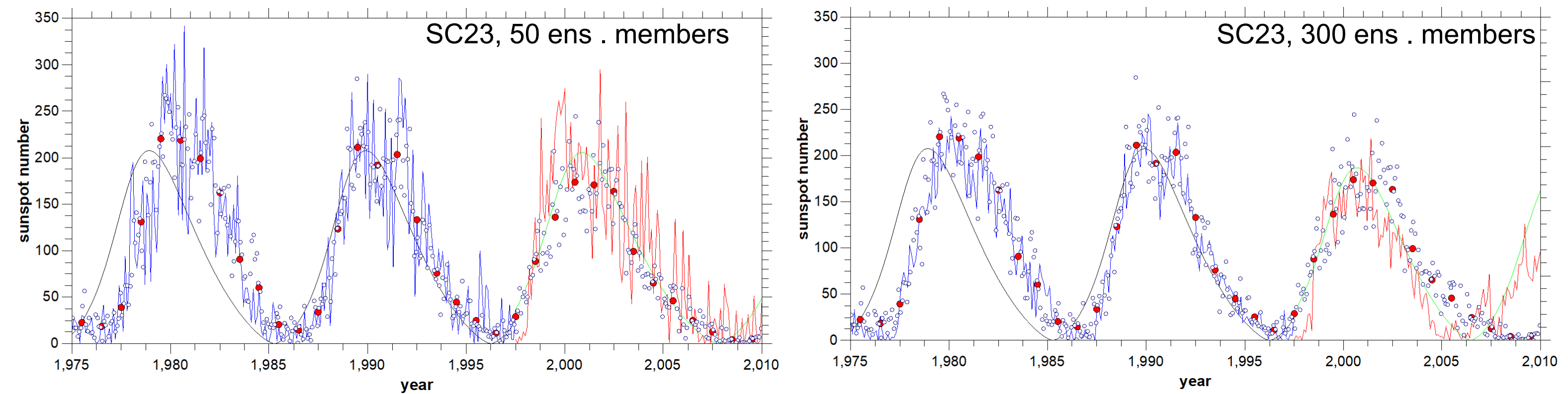

Uncertainties in Prediction of the Solar Cycle 25

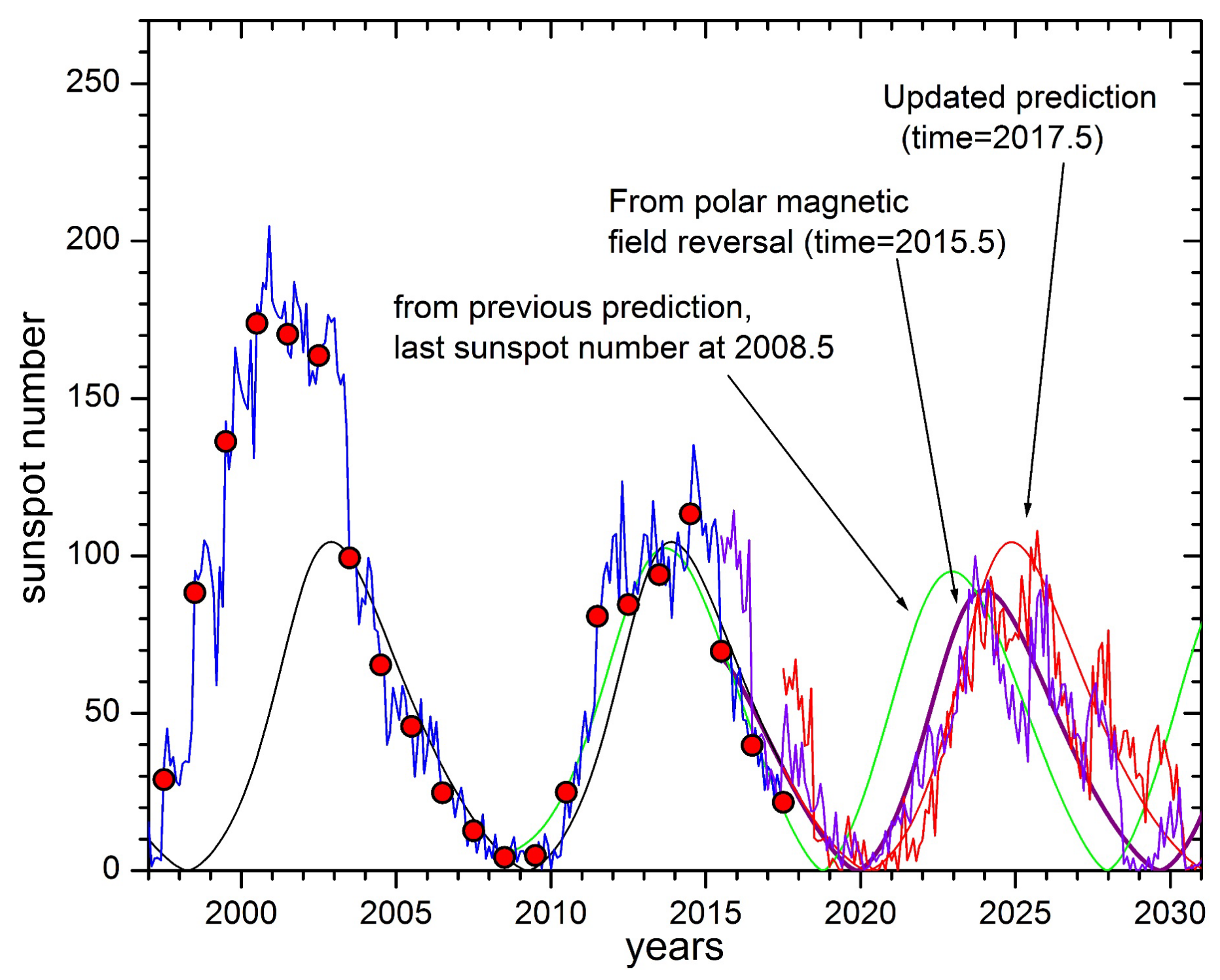

Previous experience and tests have shown that the EnKF procedure based on the dynamo model and sunspot number measurements has good predictive capabilities for estimating future solar activity in a time range from 7 - 8 years up to a whole solar cycle. However, our attempts to make predictions for a period longer than one cycle often fail due to accumulation of errors.

Testing the Prediction Capabilities

Testing the prediction capability for solar cycles 16-23. The green curves show the model reference solution. The blue curves show the best estimate of the sunspot number using the observational data (empty circles) and the model, for the previous cycles. The black curves show the model solution according to the initial conditions of the last measurement. The red curves show the prediction results.

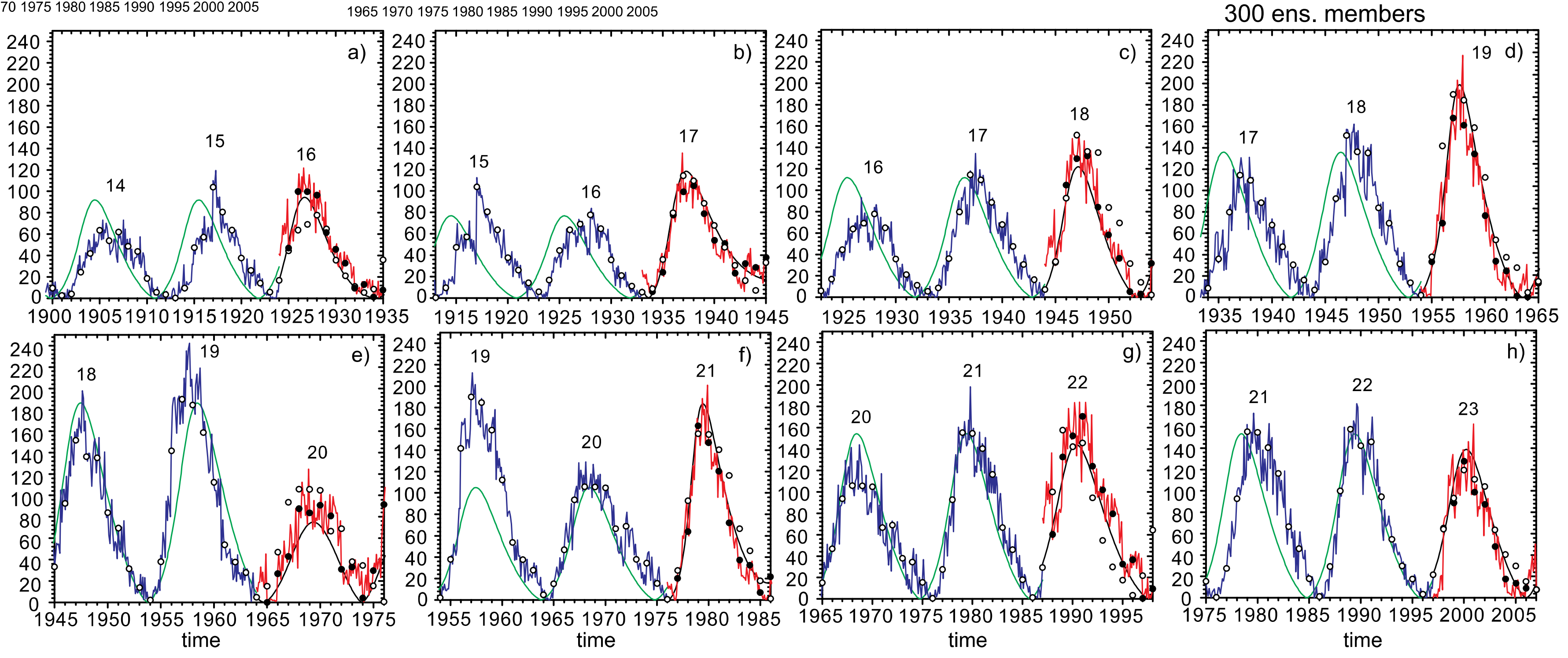

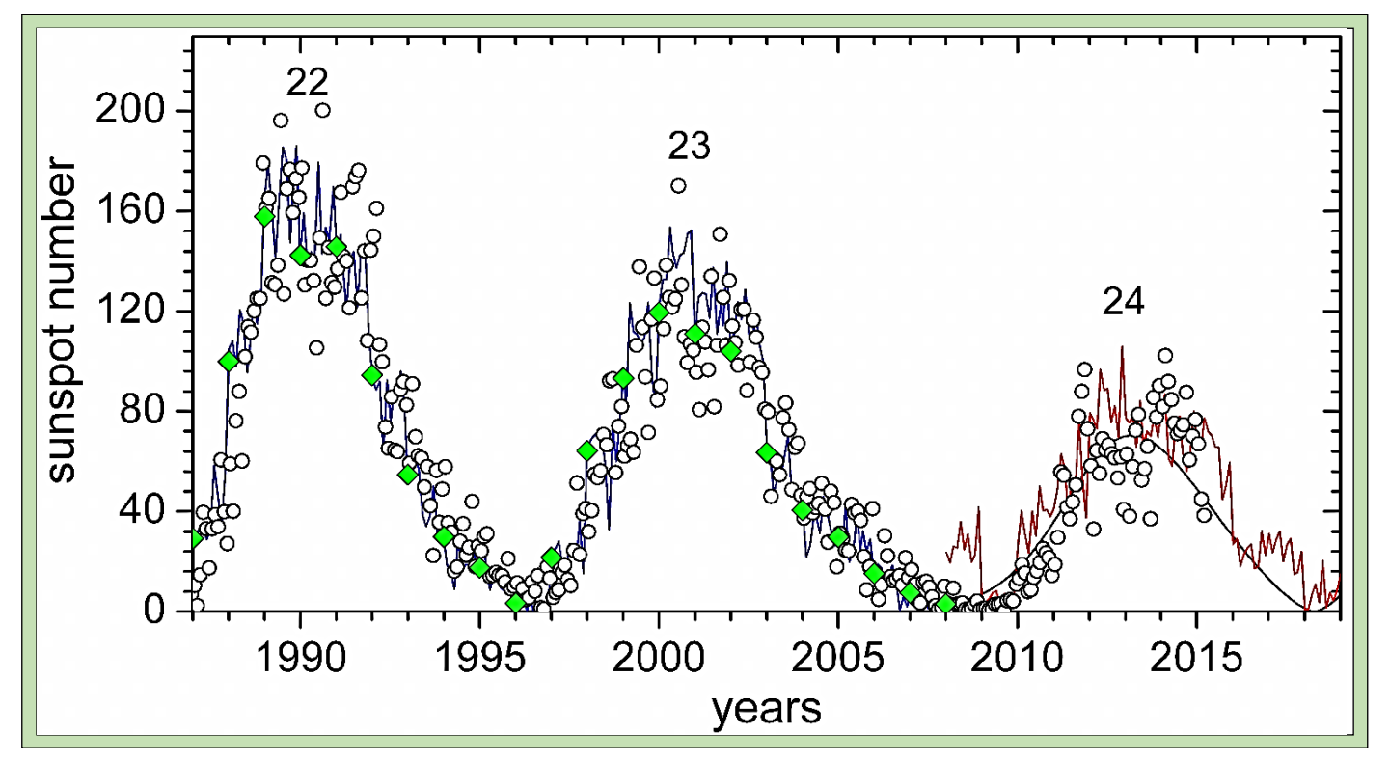

Comparison of the sunspot number prediction for Solar Cycle 24 (red curve, Kitiashvili & Kosovichev, 2008) and actual observations of monthly sunspot number. The blue curve shows the corrected dynamo solution according to annual sunspot number (green diamonds).

Conclusions

Prediction of solar cycles is one of most interesting problems closely linked to dynamo processes inside the Sun. The difficulty is due to our incomplete understanding of the physical mechanisms of the solar dynamo and also due to observational limitations that result in significant uncertainties in the initial conditions and model parameters. We have developed a relatively simple non-linear mean-field dynamo model, which nevertheless can describe essential general properties of the cycles and the observed sunspot number series (such as Waldmeier's rule). Combined with the data assimilation approach, this model provides reasonable estimates for the strength of the following solar cycles. In particular, the prediction of Cycle 24 calculated and published in 2008 is holding quite well so far. It was found that the best periods for predicting future solar cycles are during the preceding solar minimum or solar maximum. This effect is explained by the fact these periods correspond to a solar dynamo state in which the primary magnetic field components, toroidal or poloidal, change their polarity. During these periods the uncertainty of predictions is decreased because the model ensemble primarily depends on only one of the field components. However, the accuracy of the prediction is reduced when the polarity reversals are not simultaneous and occurs in the Northern and Southern hemispheres with some time delay. The reason is that the current dynamo theories are not able to model hemispheric asymmetries. This finding was unexpected and will require further investigation. Using the current observational data, prediction and prediction uncertainties have been calculated for Solar Cycle 25. The updated prediction of Cycle 25 shows that this cycle will start in about 2021, reach a maximum in 2024 - 2025, and the mean sunspot number at the maximum will be about 90 (for the v2.0 sunspot number series) with an error estimate of ~15%. The model result shows that a deep extended solar activity minimum (in about 2019-2021) is expected. Solar maximum will likely have a double peak or extended maximum activity (up to 2 – 2.5-years long).

Acknowledgement: The research is funded by the NSF SHINE program AGS-1622341